The Diffusion Tensor Reveals Gray Matter Architecture

S. N. Jespersen[1], L. A. Leigland[2], A. Cornea[3], and C. D. Kroenke[2,4]

[1]Center of Functionally Integrative Neuroscience, Aarhus University, Aarhus, Denmark, [2]Department of Behavioral Neuroscience, Oregon Health and Science University, Oregon, United States, [3]Oregon National Primate Research Center, Oregon Health and Science University, Oregon, United States, [4]Advanced Imaging Research Center, Oregon Health and Science University, Oregon, United States

Introduction: In the white matter of the brain, the anisotropy of water diffusion is thought to mainly reflect underlying tissue anisotropy in the presence of myelinated fiber tracts. Diffusion anisotropy has likewise been observed in the cortex[1], where it is believed to be imparted mainly by the anisotropic architecture of unmyelinated neurites. Here we establish a quantitative relation between the diffusion tensor and tissue cytoarchitecture as expressed by the orientation distribution of neurites in gray matter. The relation is based on a previously described model for diffusion in gray matter [2,3], but is likely to be valid in a more general setting. Experimental support from MRI diffusion measurements and quantitative histology is presented.

Theory: Following the approach in [2], diffusion in gray matter is described in terms of two components, one having cylindrical symmetry arising from diffusion in the nearly cylindrical neurites (volume fraction ν), and the other component isotropic diffusion in cell nuclei, glia cells, and extracellular space. Diffusion in the neurites is characterized by two diffusion constants, a longitudinal diffusivity D_L and transverse diffusivity D_T, whereas diffusion in the extracylindrical space is described by an effective diffusion constant D_{eff}. By analyzing the low b-value behavior of the resulting signal, we compute the diffusion tensor D and find that *its anisotropy is induced in part by the intrinsic diffusion anisotropy of the neurites, and in part by the anisotropy of the neurite architecture*. This is expressed quantitatively by the following identity

$$\frac{\nu(D_L - D_T)}{2}(\mathrm{T} - \mathrm{Tr(T)}/3) = \mathrm{D} - \mathrm{Tr(D)}/3\,, \qquad (1)$$

where T is the neurite orientation matrix [4], a rank two tensor characterizing the shape of the neurite orientation distribution function $f(\theta,\varphi)$ [2]:

$$\mathrm{T}_{ij} = \langle n_i n_j \rangle = \int_{S_2} d\Omega\, n_i n_j\, f(\theta,\varphi). \qquad (2)$$

Here the integration is over the sphere S_2, n_i refers to the i'th Cartesian component of the neurite orientation unit vector $\boldsymbol{n}$, and $\mathrm{Tr}(\cdot)$ is the matrix trace operation.

Methods: To investigate the validity of the relationship above, we acquired diffusion tensor measurements in a 31 day old female ferret. A Stejskal Tanner diffusion sequence implemented on an 11.7T Bruker magnet with two b=0 and 25 b=2500 s/mm^2 directions (icosahedral sampling scheme) was used to obtain diffusion weighted axial images from the excised brain. Diffusion gradient timings were δ = 12 ms and Δ = 21 ms, slice thickness 150 µm, voxel size 0.15 mm^3, TR≈10 s, TE = 42 ms, and number of repetitions 6. The diffusion tensor was estimated using nonlinear least-squares. In order to obtain the neurite orientation matrix, a rapid Golgi stain was applied to the right hemisphere, and 14 anatomical ROIs analyzed on 3-D high-resolution digital images (1.3 µm x 1.3 µm x 1.8 µm per voxel) recorded on a confocal light microscope using backscattered light at 633 nm. A 3-D skeletonization algorithm was applied to the confocal images, and neurite orientations determined from contiguous segments of at least 10 voxels. This yielded typically more than 1000 orientations per ROI, which subsequently were used in Eq. 2 to calculate the neurite orientation matrix. The diffusion and microscope coordinate systems were aligned by aligning the principal axes of the two tensors.

Results: The diffusion tensor and the neurite orientation matrix were diagonalized to yield three eigenvalues (λ_i and τ_i, respectively) from each of the 14 ROIs shown in Fig. 1. In each of these sets, the average eigenvalue (e.g. $\mathrm{Tr(D)}/3$) was subtracted to yield *centralized eigenvalues*. In Fig. 2, the centralized eigenvalues of the scatter matrix are plotted against the centralized eigenvalues from the diffusion tensor. There is a strong linear relationship with a linear correlation coefficient of 0.97. Note that the three centralized eigenvalues are not independent; however, a bootstrap analysis taking this constraint into account yielded p<0.005. Using Eq. 1, fractional anisotropy FA of the two tensors was shown to be related by $\nu(D_L - D_T)FA_T\sqrt{\sum_i \tau_i^2} = 2FA_D\sqrt{\sum_i \lambda_i^2}$. In Fig. 3, the fractional anisotropy of the diffusion tensor FA_D is plotted against the fractional anisotropy of the scatter matrix FA_T, and there is a significant linear correlation with a correlation coefficient of 0.71 (p<0.005). The proportionality constants in Figs. 2 and 3 are consistent with $\nu(D_L - D_T) \approx 0.8$ µm^2/ms, in agreement with previously obtained values [2, 3].

Conclusions: We developed a quantitative relation between the diffusion tensor and neurite architecture. The basic assumption underlying this result is the separation of the diffusion signal in two components, one component from a distribution of compartments with azimuthal symmetry describing diffusion in neural processes, and an isotropic component describing diffusion everywhere else. Our findings were corroborated by ROI analysis of an MRI diffusion experiment and direct histological measurements of neurite orientations obtained from histology of a postmortem ferret brain. This result aids the interpretation of the diffusion tensor in terms of tissue microstructure and architecture, and can be used e.g. in the study of plasticity and development [5].

References: 1. Neil J. J. *et al.* Radiology **209**, 57 (1998), 2. Jespersen S.N. *et al.* NeuroImage **34**, 1473 (2007) , 3. Jespersen S.N. *et al.* Proc. ISMRM 2006 and 2007, 4. Fisher N.I. *et al.* Statistical Analysis of Spherical Data, Cambridge University Press (1987), 5. Kroenke C. *et al.* Proc. ISMRM 2008.

Fig. 1

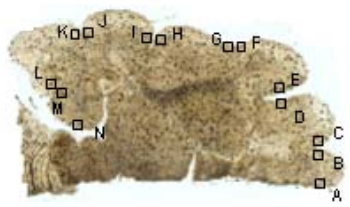

Fig. 2

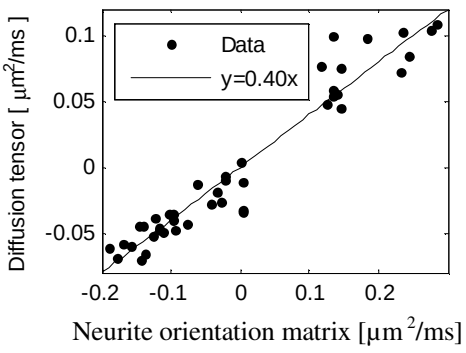

Fig. 3